Elastic and Plastic Strain Measurement in High Temperature Environment Using Laser Speckle*

F.P.Chiang
Laboratory for Experimental Mechanics Research
State University of New York at Stony Brook
Stony Brook, New York 11794-2300

SUMMARY

Two laser speckle methods are described to measure strain in high temperature environment and thermal strain caused by high temperature. Both are non-contact, non-destructive and remote sensing techniques that can be automated. The methods have different but overlapping ranges of application with one being more suitable for large plastic deformation.

INTRODUCTION

In order to measure thermal strain accurately it is paramount that the output of the measuring device not be influenced by temperature. Both mechanical and electrical strain gages require compensation schemes to overcome thermal effect. But compensation becomes difficult if not impossible when temperature extremes or large temperature gradients are involved. The situation becomes worse when the loading is a thermal shock. Optical techniques such as moire or moire interferometry require that a grating or grid be attached to the specimen surface over an area. Although it has been shown [1] that by appropriately mixing a certain ingredient into the photoresist, it can sustain temperatures up to about 560°C, at higher temperatures the grating or grid tends to disintegrate. Holographic interferometry has also been used for measuring thermal strain. However, since it is not easy to apply it to measuring in-plane strain, its application is limited.

In this paper we describe two non-contact, non-destructive and remote sensing methods of thermal strain measurement using laser speckles. In principle thermal strain up to the melting point can be measured without the aid of an auxiliary device. Other than the impingement of photons from a laser beam nothing touches the specimen. Recording can be done remotely using a telephoto lens and data analysis can be computerized.

LASER SPECKLE TECHNIQUES OF STRAIN ANALYSIS

Two laser speckle techniques are described in this article. Each has its own range of applicability and the two ranges overlap and complement each other. The first technique is the so-called speckle photography or one beam laser speckle interferometry [2,3]. When an expanded coherent laser beam illuminates a specimen surface which is optically rough (i.e.) its RMS roughness is much larger than

*Work supported by Army Research Office, Engineering Science Division Grant No. DAAL0388K0033

the wavelength of the light from the laser), multiple reflection (scattering) occurs. The reflected wavelets, being still coherent, mutually interfere to form a random interference pattern called speckles. An example of such a speckle pattern after magnification is shown in Fig.1. These are the equivalent optical displacement "gages" that are used for thermal strain measurement. Under the condition of small strain and small displacement these speckles move as if they were physically attached to the specimen surface. When they are recorded on a photographic film via a camera before and after the specimen's deformation, the superimposed speckle pattern is called a double exposure specklegram. The specklegram may be processed either in a pointwise or a full field manner. For pointwise processing, a thin laser beam impinges upon the specklegram as shown in Fig.2. Its far field diffraction pattern is a circular halo modulated by a series of uniformly distributed fringes. It can be shown [3] that the in-plane displacement vector at the probed point can be expressed as follows:

$$\bar{d} = \frac{\lambda L}{S}\bar{i} \tag{1}$$

where $\bar{i}$ is a unit vector perpendicular to the fringes, L the distance of the screen from the specklegram where the halo is received, λ the wavelength of the laser light that is used to probe the specklegram and S is the fringe spacing.

The full field processing technique uses an optical bench as shown in Fig.3. It can be shown [3] that the intensity of the diffraction spectrum displayed at the transformed plane of the first field lens is given by the following equation:

$$I(r_1, r_2) = K\cos^2 k\frac{\bar{d}\cdot\bar{r}}{L} I_s(r_1, r_2) \tag{2}$$

where $I_s(r_1, r_2)$ is the diffraction pattern of a single exposure specklegram with (r_1, r_2) being the coordinates of the spectrum plane. $k(= 2\pi/\lambda)$ is the wave number; $\bar{d}$ is the displacement vector at a point; $\bar{r}$ is a position vector at the spectrum plane; K is a proportional constant and L is the distance between the specklegram and the spectrum plane. Alternating bright and dark fringes are observed when the following condition is met:

$$\bar{d}\cdot\bar{r} = n\lambda L, \quad n = 0, \pm 1, \pm 2, ... \tag{3}$$

By placing an aperture at $\bar{r}$ and reconstructing the specimen image through the second field lens, isothetic (contours of equal displacement component) fringes similar to moire fringes are observed covering the specimen surface and they are governed by the following equation:

$$u \equiv d_x = n\lambda L/|\bar{r_x}| = nP_x, \quad n = 0, \pm 1, \pm 2, ... \tag{4}$$

$$v \equiv d_y = n\lambda L/|\bar{r_y}| = nP_y, \quad n = 0, \pm 1, \pm 2, ... \tag{5}$$

where $\bar{r_x}$ and $\bar{r_y}$ are the position vectors of the apertures sequentially located along r_1 and r_2 axes, respectively. u and v are the displacement components along x and y directions, respectively; and $P_x(= \lambda L/|\bar{r_x}|)$ and $P_y(= \lambda L/|\bar{r_y}|)$ are the equivalent "pitches" of moire gratings if they were used for the determination of strain. This technique is suitable only for the determination of small strains unless single exposure specklegram and mechanical superposition are adopted. The process has been automated as a result of our recent development of CASI (Computer Aided Speckle Interferometry) [4].

The second laser speckle technique is the so-called LSS (Laser Speckle Sensor). A schematic of this method is shown in Fig.4. A narrow laser beam impinges upon a point on the specimen surface where the strain is to be determined. The specimen surface has to be sufficiently smooth such that its scattering speckle field is fairly restricted. Upon deformation the surface roughens resulting in a more spread out speckle pattern whose autocorrelation function can be used as a means of assessing the underlying surface strain. The quantity that is most sensitive to strain is the coefficient of autocorrelation function of the speckle pattern $g(i,j)$ defined as

$$C_a[g(i,j),\delta_i,\delta j] = \frac{\sum_{i=1}^{M}\sum_{j=1}^{N} g(i,j) \times g[(i-\delta_i),(j-\delta_j)]}{\sum_{i=1}^{M}\sum_{j=1}^{N} g^2(i,j)} \tag{6}$$

where δ_i and δ_j are shifting distances along i and j directions, respectively.

One can use light scattering theory to compute the autocorrelation coefficient for various amounts of plastic strain [5]. An example is given in Fig.5 where a three dimensional view of the laser speckle field at three different levels of plastic strain in a copper alloy specimen is depicted. The corresponding experimental result is shown in Fig.6 and the agreement is quite good. The calculated autocorrelation functions for different levels of plastic strain and for different lag lengths are depicted in Figs. 7 and 8, respectively. It should be noted that the lag length is the shifting "distance" between the speckle field and its image that is used in the calculation of autocorrelation. Since the speckle field denotes the spatial frequency (see Figs. 5 and 6) of the light disturbance from the specimen surface, its dimension is in terms of lines/mm. If the area under the curve of the autocorrelation function is integrated and expressed as a function of strain, the relation can be approximated by a straight line as shown in Fig.9. Thus for plastic shear strain $\gamma \leq 3.5\%$, the linear relationship between the integrated autocorrelation coefficient and γ is

$$C_1 = 29.2\gamma - 0.04 \tag{7}$$

with an error band of 10%. For higher strains the relation is no longer linear. The broadening of the scattering speckle field becomes saturated at higher strains. In aluminum specimens we have shown that LSS can be effectively used for strains up to 20%.

APPLICATION TO THERMAL STRAIN PROBLEMS

Fig.10 shows the u and v fields' isothetics representing the thermal strain distributions of an aluminum plate at elevated temperatures. The specimen was a quarter inch thick aluminum plate of about $2' \times 2'$ in size. It was heated at the left lower corner with a propane torch. This place manifests itself as a dark spot in the pictures, especially at higher temperatures. When the torched place became red-hot at the back side, the flame was extinguished and the plate was allowed to cool naturally by thermal convection. A series of double exposure specklegrams were taken. At near the top of the plate a thermal couple was mounted to monitor the temperature change. (The wiring of the thermal couple is vaguely visible as a vertical line near the top of the picture.) The temperature reading at the time of each exposure was recorded and is indicated in the figure. A 1-joule ruby laser ($\lambda \simeq 0.69 \times 10^{-6}m$) was used to record the specklegrams. It was a pulsed laser with a pulse width of about 60 nsec. The laser only gave a single pulse and needed to be repumped after each firing. The time separation between the two pulses and the resulting temperature difference as

indicated on the picture represent the amount of cooling between the exposures. Since the thermal couple was located far away from the heat source, it is reasonable to expect that the temperature near the heat source was much higher than those indicated on the picture.

The double exposure specklegram was Fourier processed using the full-field processing scheme shown in Fig.3. Filtering apertures were placed at two orthogonal directions to yield the u- and v-field fringe patterns, respectively. A qualitative way to read the fringe pattern is as follows. Uniform strain is depicted by uniformly spaced fringes whose spacing is inversely proportional to the local average strain. Thus one can see from the pictures that at the earlier stages of thermal relaxation, the strain distribution is quite nonuniform and the strain is higher. As the convection cooling progresses the fringe becomes less dense (indicating smaller strain) and more uniform (indicating lower strain). A quantitative calculation of strain near the point where the thermal couple was located was carried out and the result is depicted in Fig.11. In the course of about 120 seconds the thermal strain has relaxed from about 0.2% to about 0.02%. The difference between horizontal and vertical normal strains also decreases with time as indicated by the gap between the two data points. A comparison of thermal strain at various temperatures for this material using data from an Alcoa Aluminum Handbook was also plotted. Within the range where comparison can be made the agreement is quite good.

Another example is the application of the laser speckle method to the determination of stress-strain relation at high temperature and high heating rate. Fig.12 is the schematic of a medium strain rate testing machine with a resistance heating attachment. Two types of testing were performed [6]. One was a soaking test at elevated temperature and the other a high heating rate test. In both tests the strain rate was kept at $10^{-1}\,\mathrm{sec}^{-1}$. Strain gages were mounted on the tensile specimen as a comparison with the laser speckle result. The ruby laser was fired once before the beginning of the test and a second time at an appropriate delay time. A camera was used to record the laser illuminated specimen. The double exposure specklegram was pointwisely processed by probing different points along the axial direction within the gage length of the specimen. The resulting Young's fringes represent the absolute displacement at the probed points between the exposures. Since the strain field is homogeneous within the gage length, the difference in displacement between two probed points divided by the separating distance is nothing but the strain. The results of the soaking test and high heating rate test are depicted in Figs.13 and 14, respectively. As can be seen from the data presented, the difference between the strain gage reading and laser speckle result is only a few percent. We have thus demonstrated the reliability of the speckle method at high temperature tests. At extreme temperatures the strain gage may fail but the laser speckle method will not. It can even be applied to specimens giving off a wide spectrum of radiation which may include the radiation of the laser. However, thermal radiation, being incoherent, does not produce speckles. To prevent thermal radiation from fogging the film, a narrow band (10Å) interference filter can be mounted on the lens of the recording camera to allow only the laser light to enter the camera.

For tests that are not repeatable, single exposure specklegram at different times can be recorded using a continuously pulsing laser (such as a copper vapor laser) and a high speed framing camera. Two single exposure specklegrams at different instances can be mechanically superimposed to yield the difference between the two stages of loading. However, the strain difference between the two cannot be too large, for otherwise decorrelation of the speckle pattern will result.

When either the strain variation or the absolute strain is large, decorrelation of laser speckle tends

to occur. In such a situation the LSS (Laser Speckle Sensor) technique should be used. The advantages of LSS technique are that only single exposure is required and speckle decorrelation will not affect the result. Currently we are in the process of applying LSS to high temperature testing and the results will be reported in the near future.

References

1. Burch, J.M. and Forno, C., "High resolution moire photography," Optical Eng vol. 21(4), 1982, pp.602-614.

2. Khetan, R.P. and Chiang, F.P., "Strain analysis by one-beam laser speckle interferometry I: Single aperture method," Applied Optics, vol. 15(9), 1976, pp. 2205-2215.

3. Chiang, F.P., "A family of 2D and 3D experimental stress analysis techniques using laser speckles," Solid Mechanics Archives, vol. 3(1), 1978, pp.1-32.

4. Chen, D.J. and Chiang, F.P., "Computer speckle interferometry," Proc. Society for Experimental Mechanics 1990 Fall Meeting, 1990., pp.49-58.

5. Dai, Y.Z. and Chiang, F.P., "Scattering from plastically roughnened surfaces and its application to mechanics," Optical Engineering, vol. 30(9), 1991, pp.1269-1276.

6. Emslie, J., Green, J., Chou, S.C. and Chiang, F.P., "The application of laser speckle interferometry to measuring strain and strain rate under dynamic conditions," Proc. Society of Experimental Mechanics, 1990 Fall Meeting, 1990, pp.59-66.

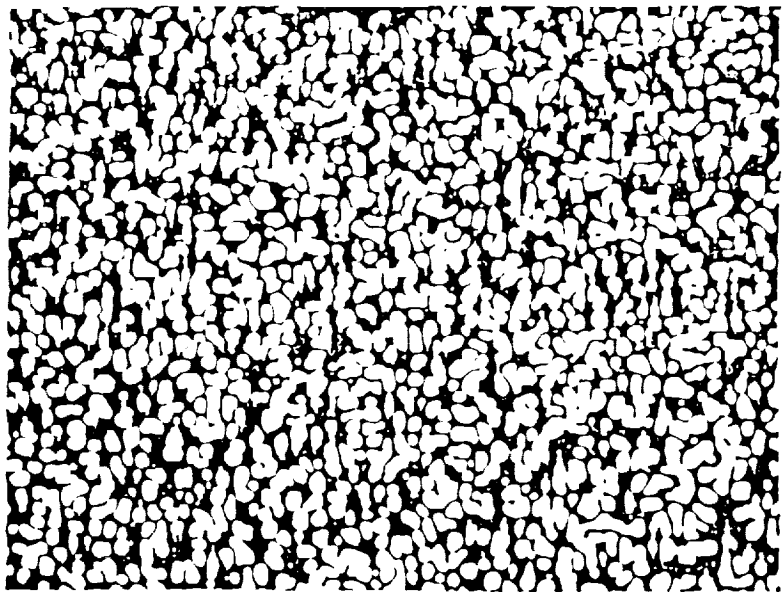

Fig.1 Typical Laser Speckle Pattern

(Original figures unavailable.)

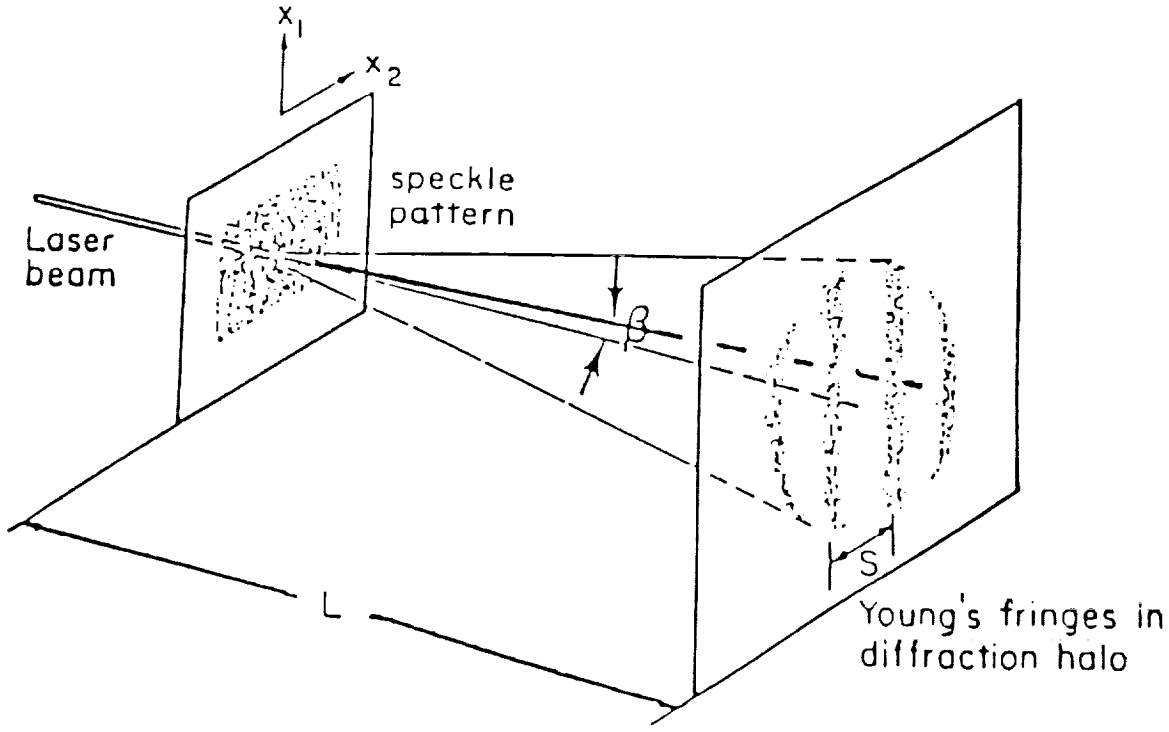

Fig.2 Pointwise Processing of Specklegram

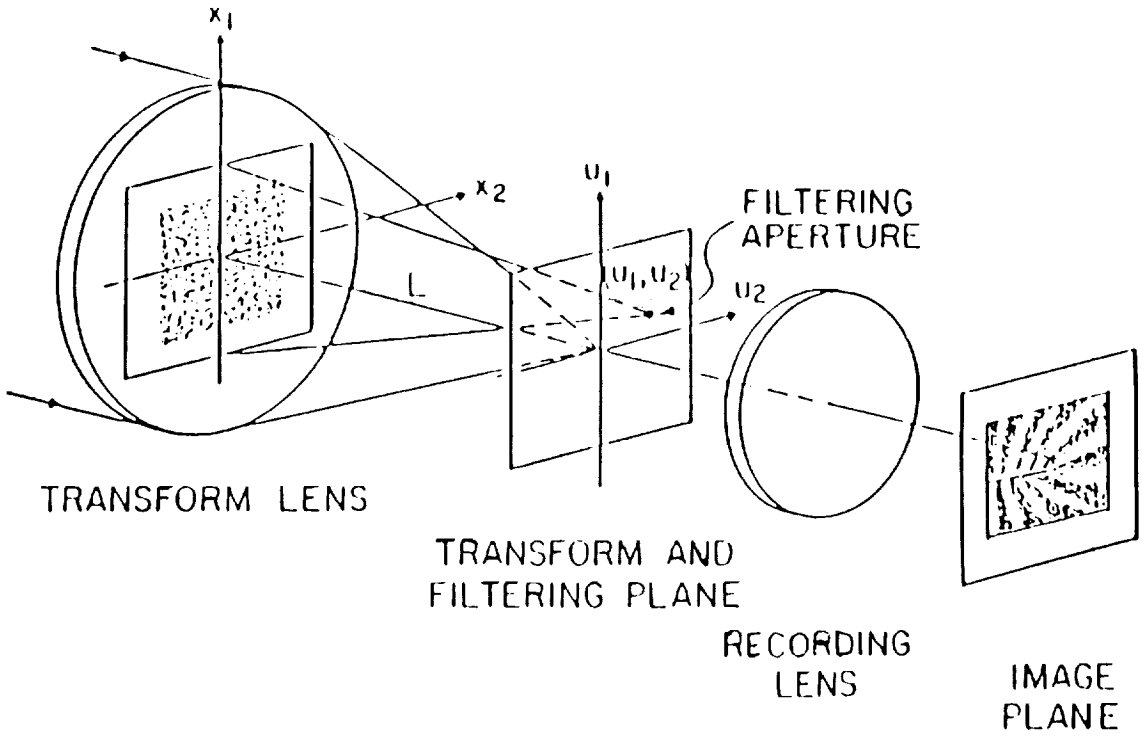

Fig.3 Full-field Processing of Specklegram

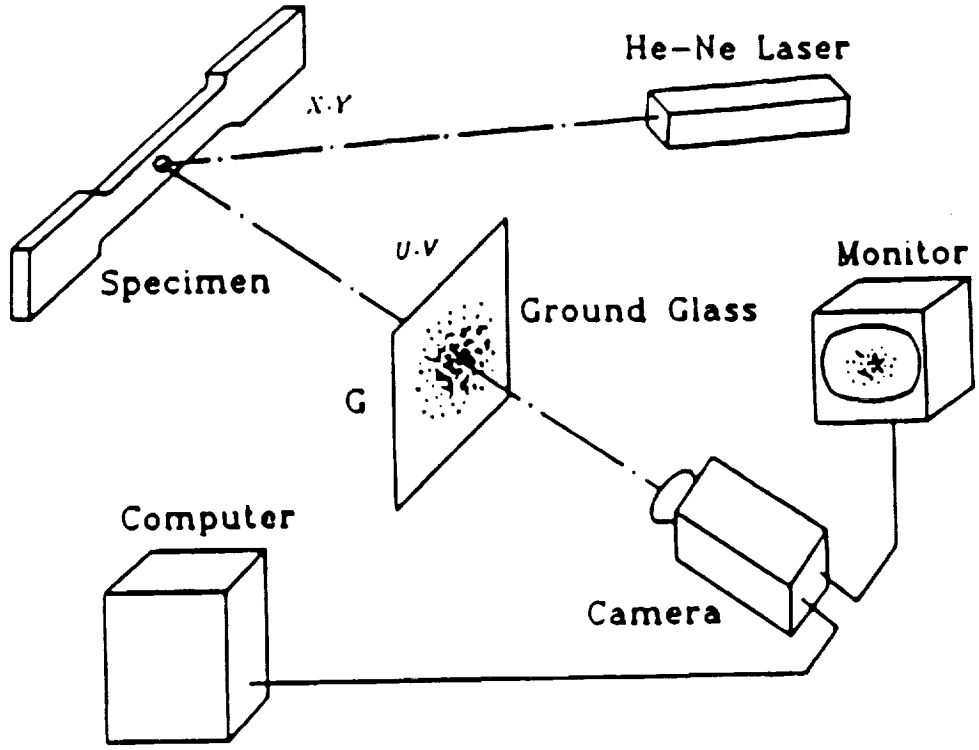

Fig.4 Schematic of LSS (Laser Speckle Sensor)

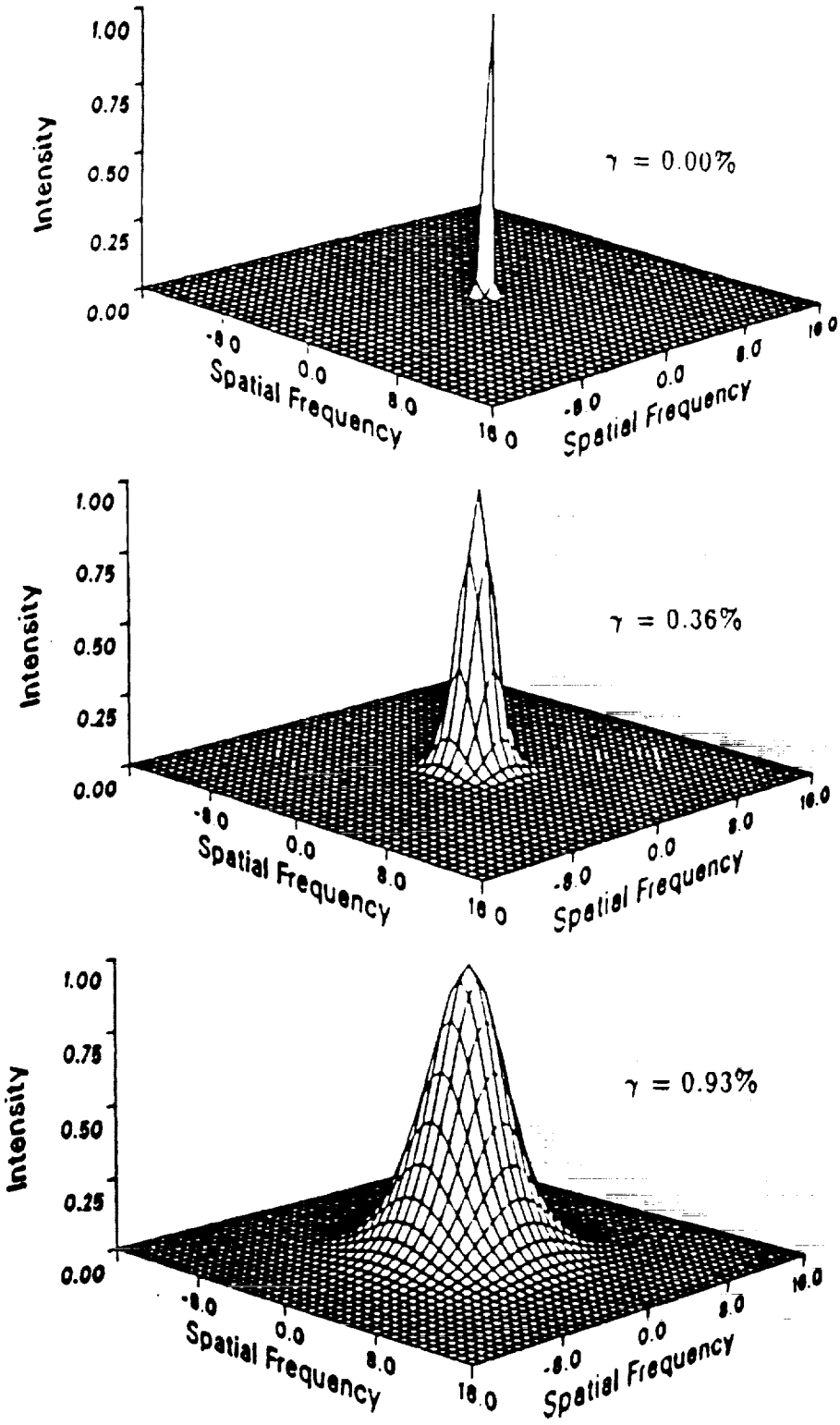

Fig.5 Theoretical Laser Speckle Field at Different Levels of Plastic Strain of a Copper Alloy Specimen

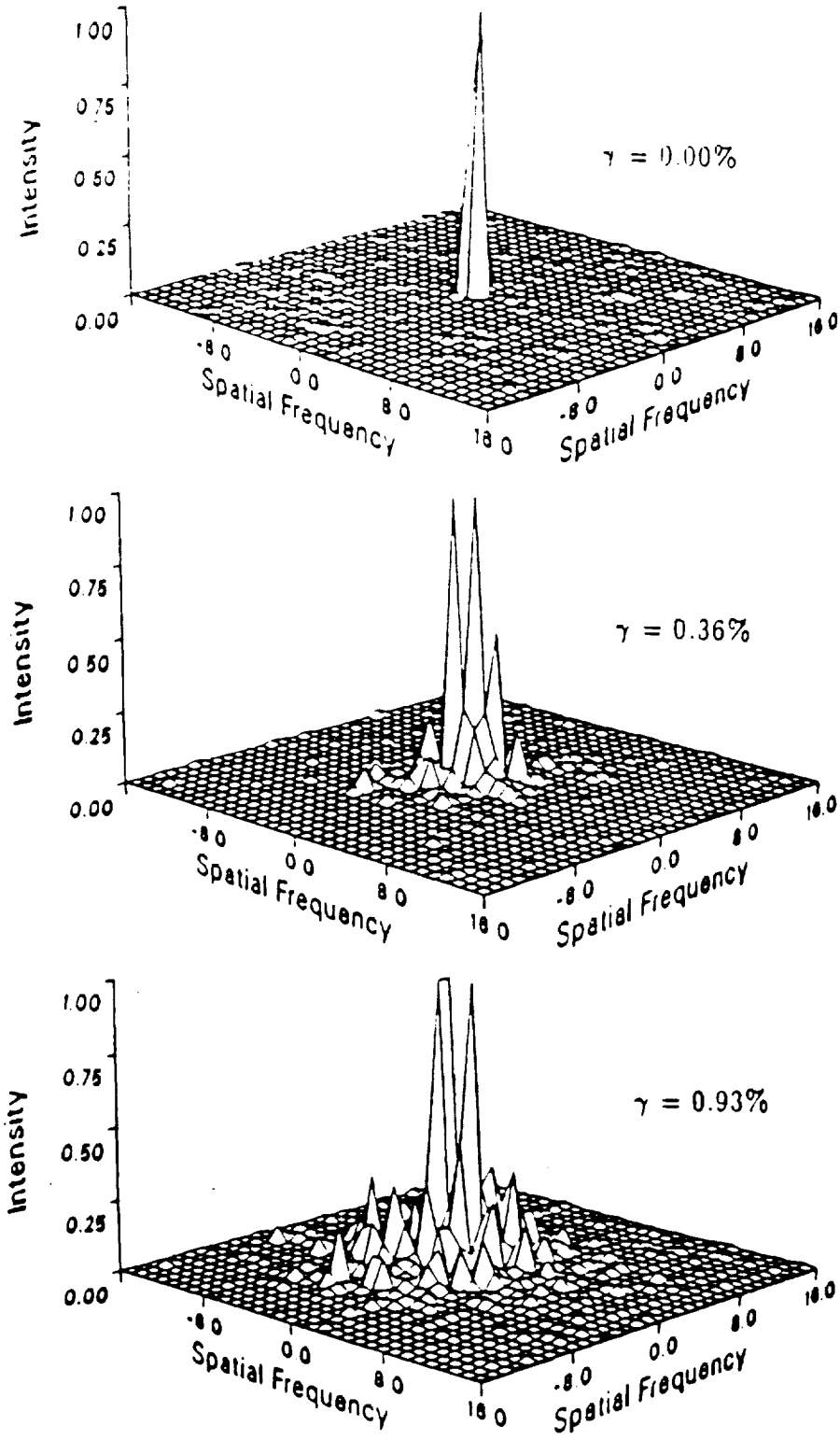

Fig.6 Experimental Laser Speckle Field at Different Levels of Plastic Strain of a Copper Alloy Specimen

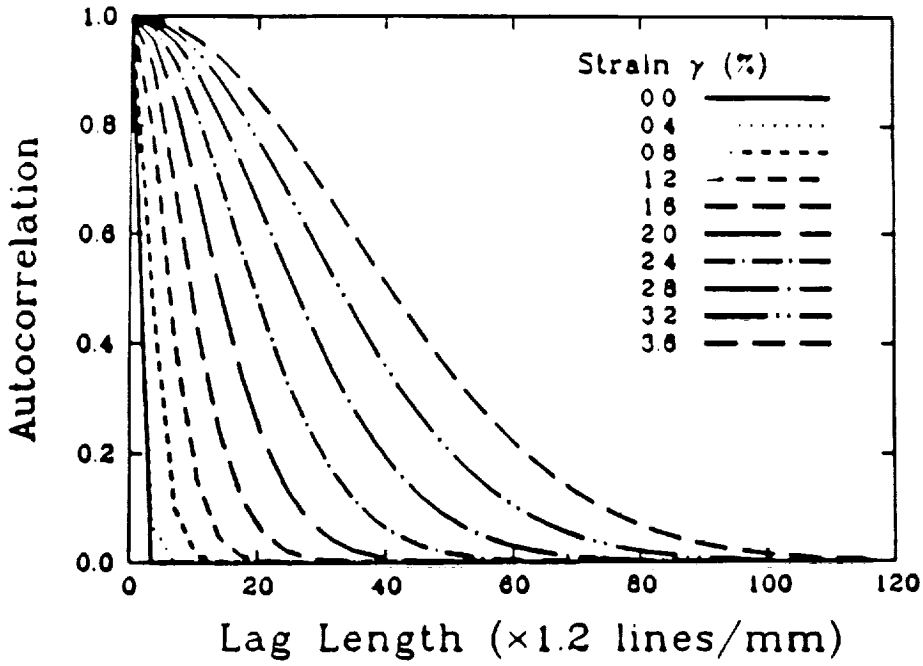

Fig.7 Theoretical Autocorrelation Function of Speckle Pattern at Different Levels of Plastic Strain

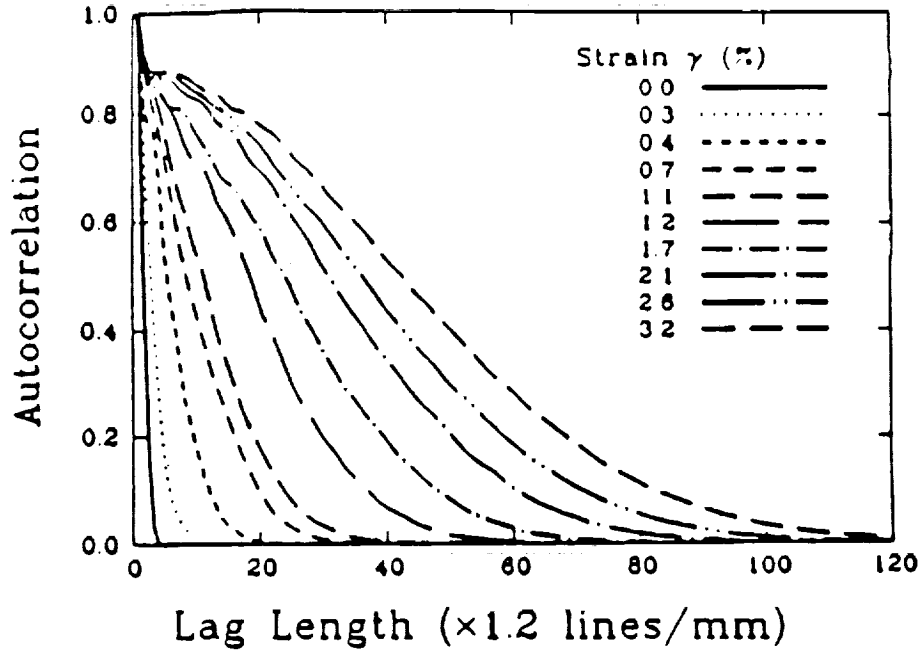

Fig.8 Experimental Autocorrelation Function of Speckle Pattern at Different Levels of Plastic Strain

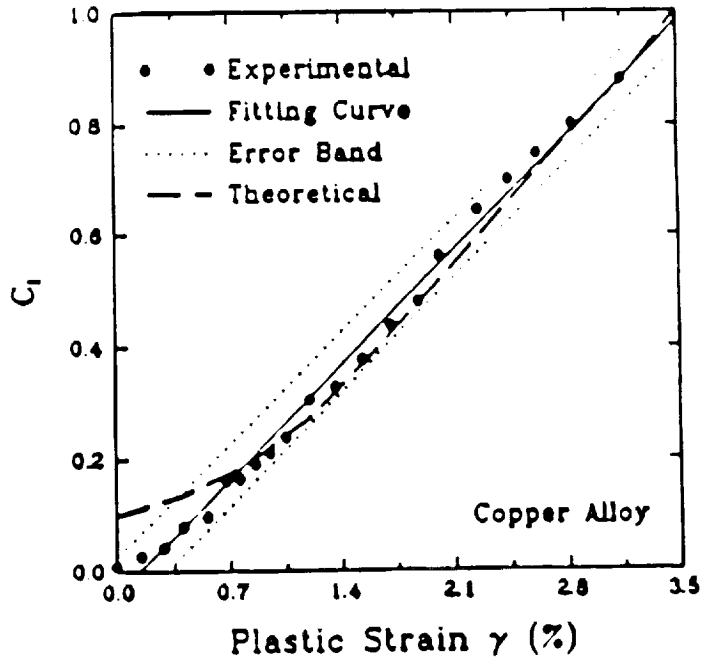

Fig.9 Integrated Autocorrelation Coefficient as a Function of Plastic Strain

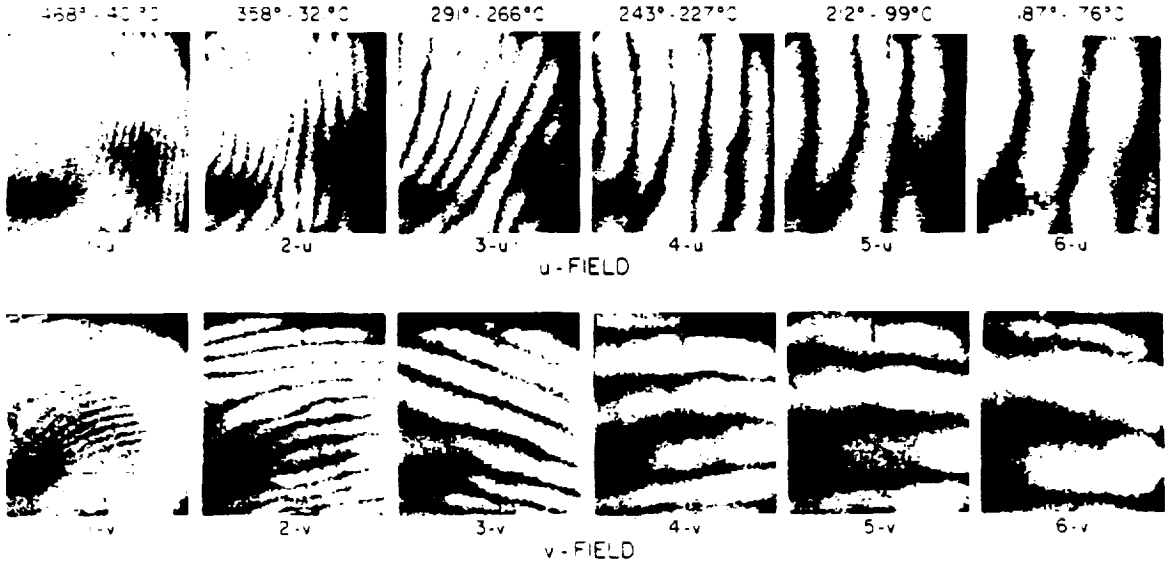

Fig.10 Distribution of Thermal Strain Relaxation of an Aluminum Plate Heated at Lower Left Corner.

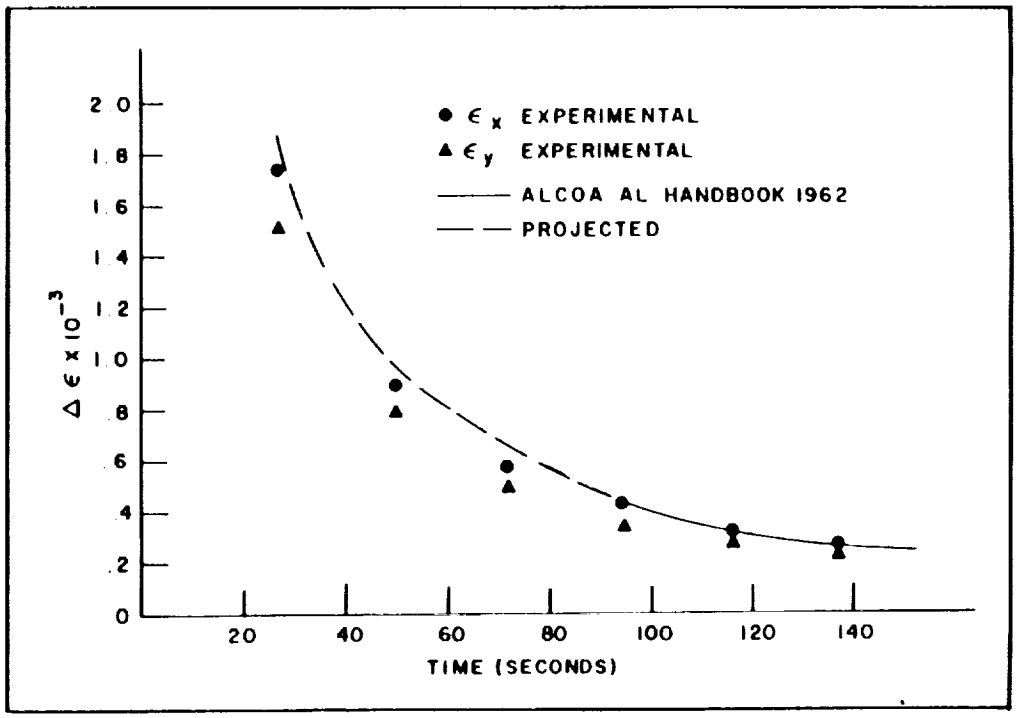

Fig.11 Thermal Strain Relaxation as a Function of Time at a Point near the Thermal Couple

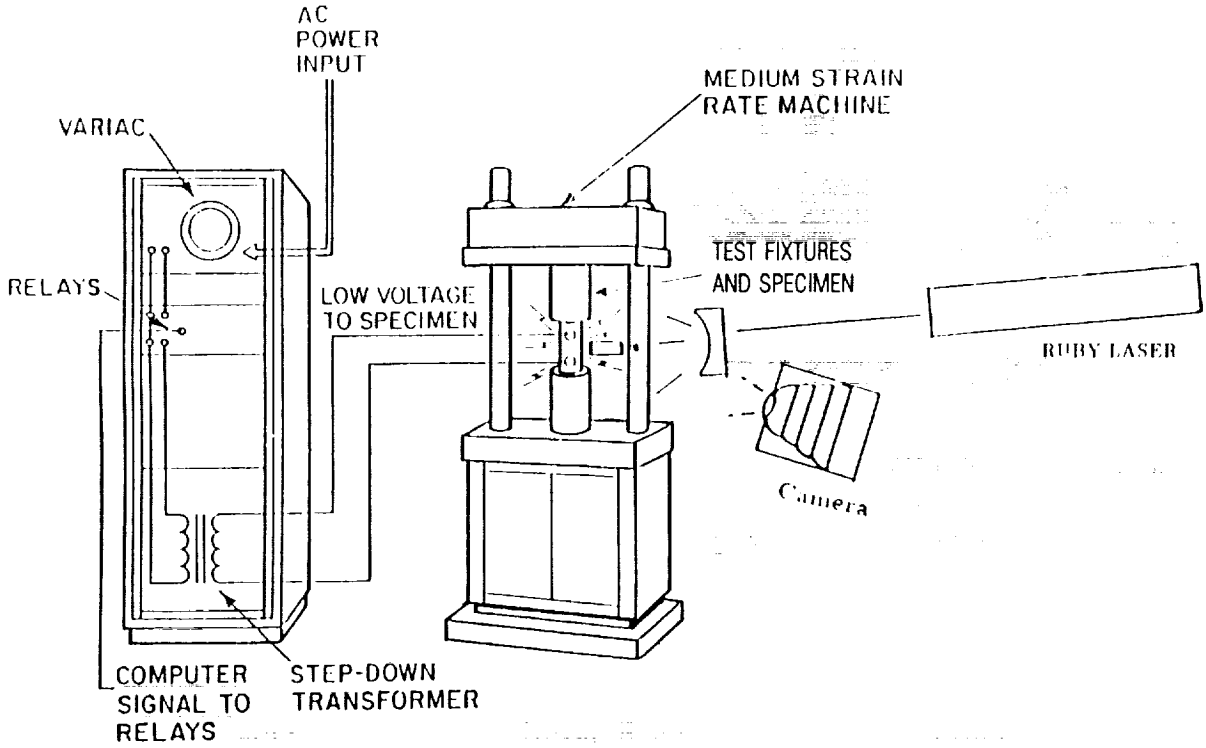

Fig.12 Medium Strain Rate Testing Using Laser Speckle Resistance Heating

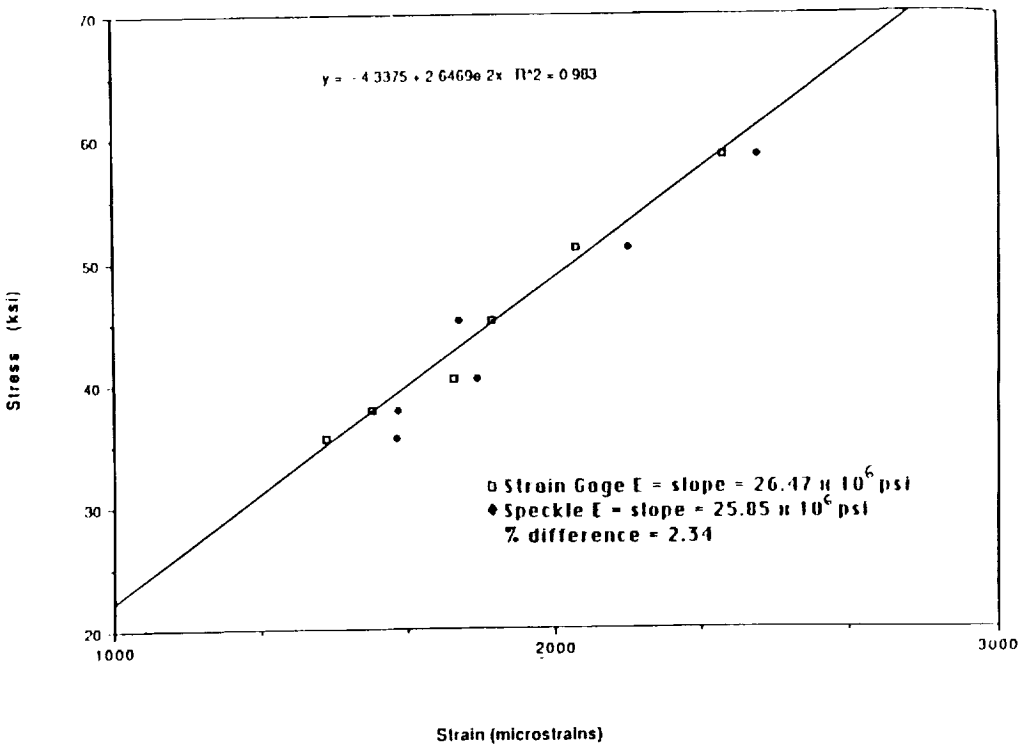

Fig.13 Results of a Soaking Test at 250°F and $\dot{\epsilon} = 10^{-1}\text{sec}^{-1}$

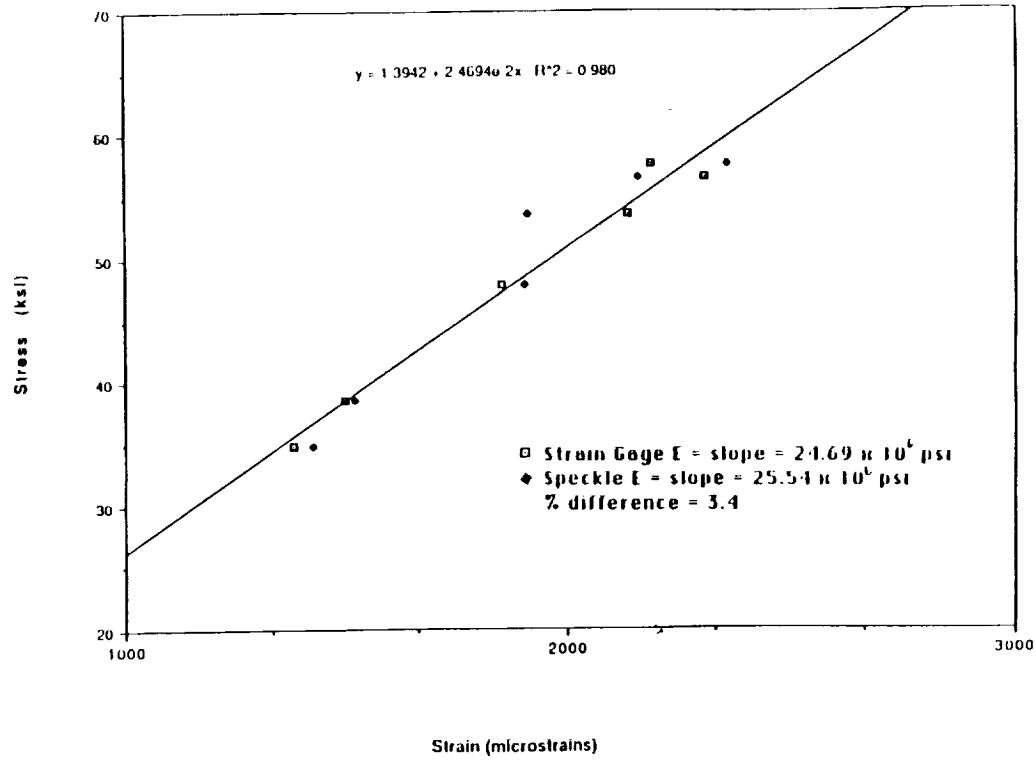

Fig.14 Results of a High Heating Rate Test at 250°F/sec. and $\dot{\epsilon} = 10^{-1}\text{sec}^{-1}$